

Published in final edited form as:

*Biochim Biophys Acta*. 2010 July ; 1803(7): 796–804. doi:10.1016/j.bbamcr.2010.03.017.

## INTERACTION BETWEEN THE MOTOR PROTEIN PRESTIN AND THE TRANSPORTER PROTEIN VAPA

Soma Sengupta<sup>a,^</sup>, Katharine K. Miller<sup>a,^</sup>, Kazuaki Homma<sup>b</sup>, Roxanne Edge<sup>b</sup>, Mary Ann Cheatham<sup>b,d</sup>, Peter Dallos<sup>b,c,d</sup>, and Jing Zheng<sup>a,d,\*</sup>

<sup>a</sup>Department of Otolaryngology, Feinberg School of Medicine, Northwestern University, 303 East Chicago Avenue, Chicago, IL 60611

<sup>b</sup>Department of Communication Sciences and Disorders, Northwestern University. Evanston, IL 60208

<sup>c</sup>Department of Neurobiology and Physiology, Northwestern University, Evanston, IL 60208

<sup>d</sup>Hugh Knowles Center for Clinical and Basic Science in Hearing and Its Disorders, Northwestern University

### SUMMARY

Prestin is the motor protein responsible for cochlear outer hair cell somatic electromotility. Eliminating this abundant basolateral membrane protein not only causes loss of frequency selectivity and hearing sensitivity, but also leads to OHC death. A membrane-based yeast two-hybrid approach was used to screen an OHC-enriched cDNA library in order to identify prestin-associated proteins. Several proteins were recognized as potential prestin partners, including vesicle-associated membrane protein associated protein A (VAPA or VAP-33). VAPA is an integral membrane protein that plays an important role in membrane trafficking, endoplasmic reticulum homeostasis, and the stress-signaling system. The connection between VAPA and prestin was confirmed through co-immunoprecipitation experiments. This new finding prompted the investigation of the interaction between VAPA and prestin in outer hair cells. By comparing VAPA expression between wild-type OHCs and OHCs derived from prestin knockout mice, we found that VAPA is expressed in OHCs and the quantity of VAPA expressed is related to the presence of prestin. In other words, less VAPA protein is found in OHCs lacking prestin. Thus, prestin appears to modify the expression of VAPA protein in OHCs. Intriguingly, more prestin protein appears at the plasma membrane when VAPA is co-expressed with prestin. These data suggest that VAPA could be involved in prestin's transportation inside OHCs and may facilitate the targeting of this abundant OHC protein to the plasma membrane.

### Keywords

Prestin; VAPA; outer hair cells; protein trafficking

---

© 2010 Elsevier B.V. All rights reserved.

\* Address correspondence to: Jing Zheng, Department of Otolaryngology, Feinberg School of Medicine, Northwestern University, 303 East Chicago Avenue, Chicago, IL 60611. Tel: 847-491-2450, Fax: 847-491-4795, jzh215@northwestern.edu

<sup>^</sup>These authors contributed equally to the work.

**Publisher's Disclaimer:** This is a PDF file of an unedited manuscript that has been accepted for publication. As a service to our customers we are providing this early version of the manuscript. The manuscript will undergo copyediting, typesetting, and review of the resulting proof before it is published in its final citable form. Please note that during the production process errors may be discovered which could affect the content, and all legal disclaimers that apply to the journal pertain.

## INTRODUCTION

Outer hair cells (OHCs) are sensory receptor cells exclusively found in mammalian cochleae. They play an essential role in increasing sensitivity and frequency selectivity of mammalian hearing (for review, see [1]). Without OHCs, hearing threshold is elevated by ~50 dB [2], frequency resolution disappears [3,4], and the ear's operation is linearized [5]. It is believed that this local mechanical amplification of the cochlear response to sound is associated with somatic electromotility [6], a unique feature of OHCs. When the voltage across the OHC's basolateral membrane (BLM) is altered, OHCs change their length [7] and stiffness [8]. OHC length is also altered if the voltage change is due to the deflection of the stereociliary bundle (the OHC's mechanosensitive organelle), as it would be with sound stimulation *in situ* [9]. The molecular basis for OHC somatic electromotility is the motor protein, prestin [10]. A series of experiments, including molecular biology, cell biology, biophysics, *in vitro* and *in vivo* physiology have demonstrated that prestin is the motor protein of OHCs and that it is required for cochlear amplification (for review, see [11,12]). For example, OHCs derived from prestin-knockout (KO) mice [13-15] or OHCs that lack fully functional prestin [12], lose somatic electromotility, and ~50 dB of hearing sensitivity, as well as frequency selectivity.

The distinct function of the OHC is associated with its several unusual cellular structural features. For instance, the plasma membrane (PM) has an uncommon lipid composition with extremely low cholesterol. Increasing cholesterol levels in the PM leads to OHC death [16]. In addition to the unique lipid composition, a high density of integral membrane proteins is found in the lateral plasma membrane [17]. In fact, the OHC's PM is densely packed with ~10 nm protein particles, with a density estimated from 2500/ $\mu\text{m}^2$  to 6000/ $\mu\text{m}^2$  [17]. How these abundant protein particles, assumed to be prestin tetramers [18], accumulate in the lateral membrane of OHCs and whether the exceptionally high protein content in the PM is related to the uncommon lipid composition or to the targeting process remain unknown. Furthermore, prestin is exclusively targeted to the BLM of polarized cells in both native cells such as OHCs [19], and non-native cells like CL4 [Zheng, L. et al., unpublished data]. Despite the fact that prestin mutants were made to study targeting sequences such as tyrosine-containing (YXXI) and di-leucine motifs [20], little is known about prestin trafficking, including the involvement of any transport protein in this process.

VAPA is an important protein involved in protein trafficking. As first discovered in *Aplysia Californica* [21], VAPA proteins are highly conserved among different species. There are two *Vap* genes in mammals: *Vapa* and *Vapb* [21]. VAPA and VAPB proteins are ubiquitously expressed integral membrane proteins associated with intracellular vesicles, the endoplasmic reticulum (ER) and microtubules [22,23]. In humans, VAPA and VAPB show 63% amino acid similarity and have common features in their structures such as a major sperm protein (MSP) domain (~120 amino acids) at their N-termini, a coiled-coil structure in the central domain, and a C-terminal transmembrane domain [23]. Mammalian VAPA is known to interact with proteins involved in regulation of sterol, lipid biosynthesis and trafficking. Proteins in this group include the FFAT (two phenylalanine in an acidic tract)-motif-containing oxysterol-binding protein (OSBP), the oxysterol-binding protein-related protein (ORP) [24], and the ceramide transport protein CERT [25]. The MSP domain of VAPA is known to interact with the FFAT motif in target proteins and is partially responsible for targeting lipid-binding proteins to the ER [26,27]. Mutation of the MSP domain (P56S) of VAPB causes the formation of large ER aggregates and is believed to be linked to late-onset amyotrophic lateral sclerosis type 8 (ALS8) [28]. In addition, VAPA is also known to interact with proteins that do not have the FFAT motif, including viral proteins whose transportation from ER to Golgi is modulated by VAPA [29], and the ER-localized transcription factor ATF6 (activating transcription factor 6) [30]. Interactions between VAPA and the other proteins not only allow the efficient transport of VAPA-associated proteins to their target locations, but also influence the associated

proteins' function. For example, over-expression of VAPA in L6 myoblasts attenuates the insulin-dependent incorporation of GLUT4 into the PM, and this effect can be suppressed by over-expression of VAMP-2 (vesicle-associated membrane protein 2), another VAPA-associated protein [31]. Thus, interaction between VAPA and an associated protein can lead to outcomes on other VAPA-associated proteins, indicating that VAPA can affect many physiological functions beyond its role as a transporting protein.

We identified VAPA as a potential partner of prestin through a high throughput membrane-based yeast two-hybrid screening [32]. In this report, we confirm interaction between VAPA and prestin in mammalian cells through co-immunoprecipitation (co-IP) experiments. By comparing VAPA expression in wild-type (WT) and prestin-KO OHCs, we discovered that lack of prestin, which is normally abundantly expressed in OHCs, affects VAPA expression. Additionally, we examined the possible role of VAPA in prestin transport inside mammalian cells.

## MATERIALS AND METHODS

### Antibodies and plasmids

Polyclonal rabbit anti-mPres antibody was raised against the carboxy terminal motif of the mouse protein as an antigen, which has been previously characterized [33]. Monoclonal anti-VAPA antibody was purchased from BD Biosciences (San Jose, CA). Anti-Frizzled3 (FZD3) antibody was purchased from Sigma (St. Louis, MO). Monoclonal anti-V5 and anti-myc antibodies were from Invitrogen (Carlsbad, CA). Monoclonal anti-GFP antibody was from BD Biosciences (San Jose, CA). Anti-Na<sup>+</sup>/K<sup>+</sup>ATPase antibody was purchased from Upstate Biotechnology, Lucerne. Anti-HIS and anti-HSC70 antibodies were purchased from Santa Cruz Biotechnology (Santa Cruz, CA). Monoclonal anti-HA antibody 12CA5 was kindly provided by Dr. Robert A. Lamb at Northwestern University. Texas Red-X phalloidin was purchased from Molecular Probes (Eugene, OR). Secondary antibodies, AlexaFluor-488 and AlexaFluor-546 conjugated anti-rabbit IgG, AlexaFluor-488 conjugated anti-mouse IgM, AlexaFluor-546 conjugated anti-mouse IgG, donkey anti-mouse IgM-HRP, and goat anti-mouse IgG-HRP were purchased from Invitrogen, Pierce (Rockford, IL) or Jackson ImmunoResearch (Bar Harbor, ME). Vectashield mounting media with DAPI was purchased from Vector (Burlingame, CA). Plasmids encoding GFP-prestin and V5-prestin were used with GFP- and V5-tags attached to the C-terminus of prestin, respectively [19,20]. pBK-NmycTecta plasmid encoding the myc- $\alpha$ -tectorin was kindly provided by Dr. K. Legan and Dr. G. Richardson of the University of Sussex. HA-HIS-VAPA plasmid was purchased from GeneCopoeia (Germantown, MA).

### Yeast two-hybrid analyses

Details of this protocol have been described before [32]. In summary, full-length mprestin (1-744 a.a.) was inserted into the bait-expression vector pAMBV4 (Dualsystems Biotech, Switzerland) with CUB-LexA-VP16 downstream of and in frame with mprestin. The bait vector carries the *LEU2* gene for auxotrophic selection. The sequence of the prestin-bait vector was confirmed through DNA sequencing. Expression of the mprestin-Cub-LexA-VP16 fusion protein was further verified by Western blot analysis with the anti-mPres antibody. Partial *Vapa* (244–993 a.a.) or partial *Fzd3* (182–356 a.a.) was inserted into the prey expressing vector pDL2-Nx (Dualsystems Biotech) with NubG upstream of and in frame with *Vapa* or *Fzd3*, respectively. The prey vector carries the *TRP1* gene for auxotrophic selection. pMBV-Alg5 is a negative control bait construct, which expresses the Cub-LexA-VP16 fusion protein in the correct orientation in the yeast membrane. The prestin-bait construct and the negative control, pMBV-Alg5, were transformed into yeast strain NMY51 (*MATa his3 $\Delta$ 200 trp1-901 leu2-3, 112 ade2 LYS2:::(lexAop)<sub>4</sub>-HIS3 ura3:::(lexAop)<sub>8</sub>-lacZ ade2:::(lexAop)<sub>8</sub>-ADE2 GAL4*)

(Dualsystems Biotech) and grown on leucine selective plates (SD-L), respectively. A *Vapa prey/Fzd3 prey* construct was transformed into prestin-bait-expressing yeast or pMBV-Alg5 expressing yeast and grown on leucine-tryptophan double selective plates (SD-LT). Positive interactions were identified by the ability of yeast to grow on leucine-tryptophan-histidine-alanine selective plates (SD-LTHA) in the presence of 2 mM 3-aminotriazole, and by  $\beta$ -galactosidase expression, indicated by the blue color observed in the presence of X-gal.

### Immunofluorescence experiments

**For cochlear tissue**—All surgical and experimental procedures were conducted in accordance with the policies of Northwestern University's Animal Care and Use Committee and the NIH Safety Guidelines. Anesthetized mice were cardiac perfused first with phosphate buffered saline (PBS) containing heparin and then fixed with 4% formaldehyde (EM grade). For cross-section samples, the cochleae were post-fixed in 4% formaldehyde for 1 hour at room temperature and placed in 10% EGTA/PBS at 4°C overnight. The decalcified cochlear samples were placed in 30% sucrose/PBS and embedded in cold OCT compound. Samples were cut in 10-20  $\mu$ m sections, placed on glass slides, fixed in 4% formaldehyde for 10 minutes and blocked at room temperature for 30 minutes in blocking solution (1% BSA, 0.2% saponin in PBS). Samples were then incubated with anti-VAPA (1:50-1:100) or anti-FZD3 (1:200) followed by incubation with anti-rabbit-IgG/anti-mouse IgM conjugated with AlexaFluor-488 (1:400) and Texas Red-X phalloidin (1:2000). Samples were then mounted on glass slides with Fluoromount-G (Southern Biotechnology Associates, Inc., Birmingham, AL) or Vectashield mounting media with DAPI and were observed using a Leica confocal system with a standard configuration DMRXE7 microscope. For whole-mount samples, EGTA and cryosectioning were omitted from the procedure.

**For transfected mammalian cells**—Plasmids encoding HA-HIS-VAPA/GFP-prestin +HA-HIS-VAPA were transiently transfected/co-transfected into HEK293T or opossum kidney (OK) cells using Effectene (Qiagen, Valencia, CA) according to the manufacturer's protocol. Approximately 28 hours post transfection, the cells were fixed with 4% formaldehyde for 10 minutes. After blocking for 1 hour, the cells were incubated with anti-HA (1:800) or anti-VAPA+anti-HIS antibody for 1 hour at room temperature. Following a brief wash, the cells were incubated with AlexaFluor-546 goat anti-mouse IgG (1:500) or AlexaFluor-546 goat anti-rabbit IgG (1:400)+AlexaFluor-488 goat anti-mouse IgM (1:400) for 30 minutes. Cells were visualized using the standard protocol described above.

### Western blot

**Whole cell lysates from transfected cells**—OK cells were transiently transfected with the plasmids encoding GFP-prestin and co-transfected with the plasmids encoding GFP-prestin +HA-HIS-VAPA, respectively. Approximately 28 hours post transfection, cells were harvested and lysed in cold lysis buffer (50mM Tris-HCl, pH 7.6, 150mM NaCl, 1% Triton X-100) supplemented with protease inhibitor cocktail (1:100) and 100  $\mu$ g/ml PMSF (phenylmethylsulfonyl fluoride). Cell debris of insoluble materials was removed by centrifugation at 10,000\*g for 15 minutes. The proteins were resolved by 7.5% NEXT-PAGE (New Electrophoresis X'PRESS Technology, AMRESCO, Solon, OH), followed by immunoblotting where GFP-prestin and HA-HIS-VAPA were detected using anti-GFP (1:1000) and anti-HA (1:2000) antibodies followed by goat anti-mouse IgG-HRP (1:5000). Signals were detected using an ECL chemiluminescent substrate (Pierce, Rockford, IL). The integrated intensity of prestin bands was measured in arbitrary units using Kodak Molecular Imaging Software (Version 5.0) as described before [34].

**Plasma membrane (PM) from transfected cells**—Transfected OK cells described above were used to isolate PM using Membrane Protein Extraction kit (BioVision, Mountain

View, CA), a procedure using aqueous two-phase partitioning [35]. Isolated PM proteins were loaded on NEXT-PAGE, and blotted with anti-GFP (1:1000) and anti-Na<sup>+</sup>/K<sup>+</sup>ATPase (1:1000), respectively. Na<sup>+</sup>/K<sup>+</sup>ATPase is a PM marker detected on OK cells [20].

**Cell lysates from cochleae**—*Cochleae* from either WT- or prestin-KO mice were collected in CelLytic mammalian tissue lysis/extraction reagent (Sigma, St Louis, MO). After homogenization, samples were incubated on ice for 2 hrs and were centrifuged at 10,000g for 10 min. Protein concentrations were measured using the Bio-Rad Protein Assay (Bio-Rad Laboratories, Hercules, CA). The same amounts of proteins from WT- and prestin-KO cochleae were loaded on NEXT-PAGE. VAPA protein was detected by anti-VAPA (1:1000). HSC70 was detected by anti-HSC70 (1:2000). HSC70 is a house-keeping protein used as an internal control.

### Co-immunoprecipitation (co-IP)

HEK293T cells were transiently co-transfected with plasmids encoding V5-prestin and HA-HIS-VAPA, as well as the negative control V5-prestin and myc- $\alpha$ -tectorin, and allowed to grow an additional 28 hours. Cell lysates (about 1.5 mg total protein) were pre-cleared by incubating with protein A sepharose (Sigma) at 4°C for 1 hour. The co-IPs were carried out by rocking pre-cleared protein lysates with either 2  $\mu$ g of anti-V5 or anti-HA antibody and Protein A Sepharose beads for either 2 hours or overnight at 4°C. Cell lysates, which had been transfected with either HA-HIS-VAPA or V5-prestin, were used as negative controls. Beads were washed three times with lysis buffer and bound proteins eluted in Laemmli buffer (with 100 mM DTT). The proteins were resolved by 7.5% NEXT-PAGE. Standard protocols for Western blot, primary (anti-HA, 1:2000; anti-V5, 1:5000; anti-myc, 1:5000) and secondary antibody incubation, and detection by ECL were then followed.

## RESULTS

### Yeast two-hybrid analysis identifies VAPA as a potential interacting partner of prestin

VAPA was identified as a potential prestin partner through a membrane-based yeast two-hybrid screen [32]. In order to eliminate possible false positives, commonly found in yeast two-hybrid assays, the interaction between prestin-bait and VAPA-prey was further tested. SD-LTHA selective plates not only produce both the bait and prey proteins but also show an interaction between them. The yeast co-expressing VAPA-prey and prestin-bait (Fig. S1B) grew on SD-LTHA selective plates and turned blue when tested for the activation of the *lacZ* gene (data not shown). However, yeast expressing control-bait and VAPA-prey showed no growth (Fig. S1A). In other words, VAPA-prey interacts with prestin-bait but not with the control-bait, indicating that VAPA is a potential interacting partner of prestin.

### VAPA interacts with prestin in mammalian cells

The detection of an interaction between prestin and VAPA in yeast does not necessarily mean that the same interaction will occur in mammalian cells, as yeast and mammalian cells differ in many ways. Therefore, interaction between prestin and VAPA was investigated in mammalian cells by co-IP experiments. Plasmids encoding V5-prestin and HA-HIS-VAPA were transiently co-transfected into HEK293T cells. As a negative control, plasmids encoding V5-prestin and myc- $\alpha$ -tectorin were transiently co-transfected into the same cell line. As  $\alpha$ -tectorin localizes to the tectorial membrane (an acellular gel) and prestin is located at the basolateral membrane of OHCs, an interaction between them is unlikely *in situ*. Therefore,  $\alpha$ -tectorin was used as a negative control. Cell lysates were incubated with anti-V5/anti-HA antibody and protein A-sepharose and eluted proteins were run on NEXT gel followed by blotting with either anti-HA, anti-V5 or anti-myc antibody. As shown in Fig. 1A (left), VAPA was co-immunoprecipitated with prestin when anti-V5 was used to pull down V5-prestin



protein and its associated proteins. In contrast, no VAPA signal was observed in IPs of VAPA-only expressing lysate (lane 4 in Fig. 1A). As expected, eluted proteins also contain prestin (Fig. 1A, right). Likewise, prestin was co-immunoprecipitated with HA-tagged VAPA when anti-HA was used to pull down HA-VAPA protein and its associated proteins (lane 4 in Fig. 1B, left). The eluted proteins also contain VAPA as expected (Fig. 1B, right). Together, these data confirm the interaction between VAPA and prestin in mammalian cells. For the negative control,  $\alpha$ -tectorin was not co-immunoprecipitated with prestin when anti-V5 was used to pull down V5-prestin proteins (Fig. 1C, left) although abundant prestin protein was eluted from anti-V5-beads (Fig. 1C, right). As expected, both prestin (Fig. 1C, right) and  $\alpha$ -tectorin (Fig. 1C, left) were present in the flow-through. These data indicate that the lack of co-IP between prestin and  $\alpha$ -tectorin is not due to lack of prestin and  $\alpha$ -tectorin proteins. Hence, these data demonstrate that the interaction between VAPA and prestin is specific.

### VAPA and prestin co-localize in OHCs

Our data demonstrate that VAPA interacts with prestin in both yeast and mammalian cells. Since VAPA is an important protein involved in protein trafficking [25-29], we suspected that VAPA was involved in prestin's transportation in OHCs, where prestin proteins are expressed. Before investigating VAPA protein expression in the cochlea, the specificity of anti-VAPA antibody was tested in HEK 293T cells transiently transfected with HA-HIS-VAPA plasmid using immunofluorescence. The anti-VAPA staining pattern in HEK293T is similar to that of anti-HIS, which recognizes HIS antigen attached to VAPA protein (as shown in Fig S2). These data suggest that anti-VAPA antibody can recognize VAPA protein. Using this antibody, we investigated expression patterns of prestin and VAPA in P5 WT-mice. As shown in Fig 2, VAPA is widely expressed in the organ of Corti, while prestin is specifically located in OHCs. Co-localization of VAPA and prestin staining appears in yellow color as indicated by the arrowhead. For better examination, the image corresponding to the location marked with the arrowhead is given at a higher magnification (right corner in Fig 2K). The observation that VAPA co-localizes with some prestin in OHCs is consistent with the function of a cargo carrier. However, as a transport protein, VAPA does not always co-localize with its associated proteins, including prestin.

### VAPA protein content in OHCs alters with prestin expression

Prestin is abundantly expressed only in OHCs, and the time course of prestin mRNA and protein synthesis corresponds to the emergence of somatic motility in OHCs [10,36]. Prestin protein is highly produced during the first two weeks of development, more specifically from around P5 until about P13 [36]. If VAPA is indeed involved in the transport of prestin to the PM, in addition to its other cellular functions, VAPA expression should increase during the time that prestin is most heavily produced. In order to investigate the effect of prestin on VAPA expression, we examined VAPA expression by Western blot using cochleae derived from P10 and P13 WT- and prestin-KO mice. As shown in Fig 3A, intensities of the VAPA protein band in both P10 and P13 prestin-KO cochleae is less compared to P10 and P13 WT cochleae, while intensities of the house-keeping protein HSC70 bands are similar among WT- and prestin-KO samples. The integrated intensities of protein bands for VAPA and HSC70 in WT- and prestin-KO samples were measured in arbitrary units using Kodak Molecular Imaging Software. Fig 3B shows the comparison of VAPA expression in WT- and prestin-KO cochlea where the band intensity of VAPA is divided by the HSC70 intensities for the respective cochlea. VAPA expression in WT-cochleae is significantly more than that in prestin-KO cochleae ( $p=0.01$ ,  $n=2$ ). Thus, it appears that VAPA expression in cochleae is influenced by the presence of prestin protein.

Since prestin is an OHC specific protein (Fig. 2), we focused on whether this change of VAPA protein expression is present in OHCs. Immunofluorescence images of individual OHCs

selected from different locations along the P13 cochlea are shown in Fig. 3C. Higher VAPA expression is seen (denoted by green color) in WT as compared to prestin-KO OHCs, whereas actin staining (denoted by red color of Texas Red-X phalloidin) is unaltered. The area between the cuticular plate and the OHC nucleus, as outlined in one of the WT OHCs in Fig. 3C, was measured in pixels using NIH Image J and the green spots, assumed to be VAPA-containing vesicles, were counted manually within that area. Counts made between the cuticular plate and the nucleus were compared between WT- and KO-OHCs. Significantly, more green spots per measured area were found in the OHCs from WT-mice, independent of cochlear location ( $p=0.0001$ ) as shown in Fig. 3D. The green spots located around the synaptic region were not quantified due to the difficulty in separating spots located in OHCs from those found in Deiters' cells.

VAPA is not an OHC-specific protein. In fact, VAPA is widely expressed in different cells in the organ of Corti. Fig. 4 shows radial views of the organ of Corti derived from both P13 WT- and prestin-KO mice. Both VAPA and prestin are synthesized in WT-OHCs at this time. Fig. 4a and d indicate that VAPA is not only an OHC specific protein. Green spots, designating VAPA protein, are also found in supporting cells such as Deiters' cells (D), pillar cells (P), and neuronal termini in both WT- and prestin-KO cochleae. As a control, Fig. 4g shows no green spots when anti-VAPA antibody was not used, indicating that the green spots in Fig. 4a and d specifically denote VAPA protein. As shown in Fig. 4a and d, the intensities and distribution patterns of green VAPA spots in these supporting cells are similar in WT and prestin-KO cochleae. Like OHCs, green spots were measured in fixed area of supporting cells of WT- and KO-cochlea in Fig 4a and 4d. As shown in Fig 3D, there is no significant difference ( $p=0.65$ , approximately 300 spots analyzed from two sets of organ of Corti) in VAPA protein in supporting cells (SC) derived from WT- and prestin-KO organ of Corti. These results demonstrate that VAPA expression is altered only by prestin in OHCs but not in supporting cells where prestin is absent.

As OHC death is associated with lack of prestin [37], it is possible that the reduced VAPA expression observed in prestin-KO OHCs is due to their potentially unhealthy condition. Therefore, we compared the expression of another potential prestin partner, FZD3 [32], in OHCs from both WT- and prestin-KO mice. FZD3 is suggested to be involved in the planar orientation of hair bundles in hair cells [38,39]. At P0, when no prestin is expressed in OHCs [10], FZD3 protein (green color) was found asymmetrically at one proximal edge in both WT- and prestin-KO OHCs as indicated by the white arrowheads (Fig. 5), similar to the distributions reported previously [38,39]. In adults, however, these asymmetrical FZD3 distributions disappear and a reduced homogenous FZD3 staining is found in cytoplasm, as shown in Fig. 6A. We have compared FZD3 protein expression at different developmental stages and found no obvious difference between WT and prestin-KO cochleae. To be precise, we compared FZD3 protein expression between WT and prestin-KO cochleae by measuring mean intensities of FZD3-fluorescence in the cytoplasm using NIH Image J. The area of each cell was selected and measured for mean intensity in arbitrary units. An area of background from each image was also selected and measured. The intensity of the background was then subtracted from the mean intensity. The average intensity of FZD3 from both WT and prestin-KO was then calculated and compared. As shown in Fig. 6B, there is no significant difference in FZD3 intensity between WT and prestin-KO OHCs, ( $p=0.11$ , WT  $n=15$ , KO  $n=14$ ). Hence, unlike VAPA, FZD3 expression in OHCs is not prestin-dependent. Together, data from experimental and control conditions suggest that the connection between VAPA and prestin is indeed real.

### VAPA increases prestin membrane targeting

Since the major function of VAPA is involvement in protein transportation, and we have demonstrated that prestin interacts with VAPA and affects VAPA's expression level in OHCs

(Fig 1, 2, 3 and 4), we suspected that VAPA is involved in prestin trafficking in OHCs. Unfortunately, a *Vapa* knockout mouse is not available, so we were unable to study the influence of VAPA on prestin's function *in vivo*. Therefore, we chose a heterogenous system to investigate VAPA's influence on prestin. OK cells, like OHCs, are polarized cells. They also have a larger cytoplasm-to-nucleus ratio, allowing better determination of intracellular localization of the transfected protein. OK cells were transiently transfected with plasmids encoding GFP-prestin and HA-HIS-VAPA cDNAs. As shown in Fig. 7D, VAPA and prestin were partially co-localized in the PM of mammalian cell, similar to the pattern observed in P5 OHCs (Fig. 2). Since protein trafficking is one of VAPA's major functions, it is likely that this partial co-localization comes from involvement of VAPA in prestin transport. To examine the involvement of VAPA in prestin transport, we compared cells transfected only with GFP-prestin and those co-transfected with both GFP-prestin and HA-HIS-VAPA. Since cells with the single transfection and co-transfection may have different levels of prestin expression, we first compared amounts of prestin synthesized in these cells. As shown in Fig. 7E, both samples have three prestin bands representing the non-glycosylated prestin monomer (the lowest band), the N-glycosylated prestin monomer (the middle band) and prestin's dimer (the upper band) as described before [33]. The integrated intensities of all prestin bands in each sample were measured in arbitrary units using Kodak ID Image Analysis software [34]. There was no significant difference ( $p=0.55$ ,  $n=3$ ) in the amount of prestin protein synthesized in the single transfected versus the co-transfected cells. However, the difference in prestin distribution patterns between cells that express only GFP-prestin and cells that express both GFP-prestin and VAPA is substantial. As shown in Fig. 7A, in many of the prestin-only transfected cells, prestin is stacked intracellularly with no prestin in the plasma membrane, whereas in co-transfected cells (Fig. 7B-D), substantial amounts of prestin are present in the PM along with intracellular structures. In other words, more prestin proteins are delivered into the PM in the presence of over-expressed VAPA, indicating a role for VAPA in prestin transport. To be more precise, we subjectively classified cells into two groups: cells with prestin targeted to the PM, and cells without prestin staining in the PM. We then graded the cells (approximately 100 to 200 cells for each experiment) randomly from at least three transfection experiments. As shown in Fig. 7F, a majority of cells expressing GFP-prestin alone (65%) did not have green prestin staining in their PM. In contrast, most cells expressing both GFP-prestin and VAPA did show prestin staining at their PM (60%). There was a significant difference ( $p=0.02$ ,  $n=3$ ) in the percentage of cells containing prestin in the PM between single and co-transfected cells. To restate, more prestin protein was delivered into the PM when VAPA was co-expressed with prestin. Since similar levels of prestin were expressed in both single- and co-transfected cells (Fig. 7E), we rule out the possibility that VAPA expression may simply alter prestin protein-expressing levels rather than directly affecting protein trafficking. Thus, the presence of over-expressed VAPA proteins seems to help prestin successfully translocate into the PM.

To further support this claim, we also used a biochemical method to isolate the PM from OK cells that were transfected with either HA-HIS-VAPA+GFP-prestin or those with  $\alpha$ -tectorin +GFP-prestin. As shown in Fig 7G, more prestin is found in the PM of VAPA+prestin-transfected cells compared to that of  $\alpha$ -tectorin+prestin-transfected cell.  $\text{Na}^+/\text{K}^+$ ATPase was used as the PM marker. These data further support the involvement of VAPA in prestin transport. Two different methods, biochemical and cellular biology, demonstrate that VAPA increases prestin delivery to the PM in an *in vitro* system.

## DISCUSSION

Prestin is a unique molecular-motor protein exclusively expressed in the PM of OHCs in the organ of Corti of the mammalian cochlea. Due to its contribution to the OHCs' characteristic somatic electromotility, it is of interest to find proteins that interact with prestin. However, very few prestin-associated proteins have been described [40]. This is the first report identifying



VAPA as an interacting partner for prestin in OHCs. Although this interaction was found in yeast, it was confirmed in mammalian cells using both co-localization and co-IP experiments, and further verified in OHCs. We have also shown that in mammalian cells the translocation of over-expressed prestin to the PM, which is analogous to the abundant prestin expressed in OHCs, increases in the presence of over-expressed VAPA. This gives evidence of the involvement of VAPA in prestin translocation.

Among the interacting partners of prestin, identified by the yeast two-hybrid screen, two-proteins, FZD3 and VAPA were studied here. We have shown that while FZD3 expression is unaffected in prestin-KO OHCs, the amount of VAPA expression is somehow related to the presence of prestin proteins, inasmuch as fewer VAPA proteins are found in prestin-KO OHCs. It thus appears that prestin regulates the expression of VAPA protein in OHCs. One possible explanation might be that abolishing the expression of such an abundant protein, like prestin in OHCs, could result in a reduced demand for transport proteins, such as VAPA. However, how prestin regulates VAPA's expression remains unknown.

From previous studies, it is known that VAPA is involved in regulating lipid transfer at the ER-Golgi membrane contact sites by directly binding certain lipid-transfer and/or lipid-binding proteins, thereby controlling cholesterol and sphingomyelin production. Our data provide another example of VAPA's involvement in protein transport. Further experiments are needed to investigate where and how VAPA is involved in prestin transport. For now, one cannot rule out the possible presence of an intermediate protein in this transportation process. Commonly, the MSP domain of VAPA is known to interact with the FFAT-motif in the target protein. Interestingly, our results show strong binding (as shown by both yeast two-hybrid and co-IP analyses) between VAPA and prestin, yet there is no apparent FFAT-motif in prestin. So, in addition to Norwalk virus nonstructural protein p48 [29], prestin is another example of non FFAT-containing proteins that bind to VAPA. As we used full-length prestin as the bait for selecting prey, it is difficult to predict which domain of prestin is involved in binding to VAPA. According to sequence analysis, binding between prestin and VAPA does not involve the N-terminus MSP domain of VAPA. One may broadly speculate that the coiled-coil structure (the central domain) and/or the intracellular membrane anchor at the C-terminus of VAPA are most likely to be involved in the interaction with prestin.

Recent data suggest that VAP family proteins are not simply cargo carriers. They are involved in multiple cellular functions, including membrane trafficking, cytoskeleton association and membrane docking interactions for ER-localized transcription factor ATF6 [30]. A single missense mutation (P56S) within the human *Vapb* gene causes ALS8, due to the formation of endogenous VAPB aggregates, which recruit both WT VAPA and VAPB. Consequently, the reduction in cytosolic VAP level results in the disruption of binding between WT VAP-proteins and FFAT-motif-containing proteins, eventually leading to motor neuron degeneration [28]. In addition, VAPA and VAPB can interact with and modulate the activity of ATF6 [30], a sensor for the UPR (unfolded-protein response) signaling cascades expressed in response to cellular stress and possibly triggering apoptosis [41].

In conclusion, our data demonstrate that VAPA is a novel interacting partner for prestin and may be involved in prestin translocation to the plasma membrane. Prestin trafficking in OHCs could involve many proteins, and VAPA may be one of them. Further studies are required to understand the molecular mechanism of how prestin regulates VAPA expression, and how VAPA regulates membrane composition in OHCs. Understanding the activation mechanism could eventually help us prevent OHC loss, which is the most common sensory defect, affecting millions of people ranging from newborns to the elderly.

## Supplementary Material

Refer to Web version on PubMed Central for supplementary material.

## Acknowledgments

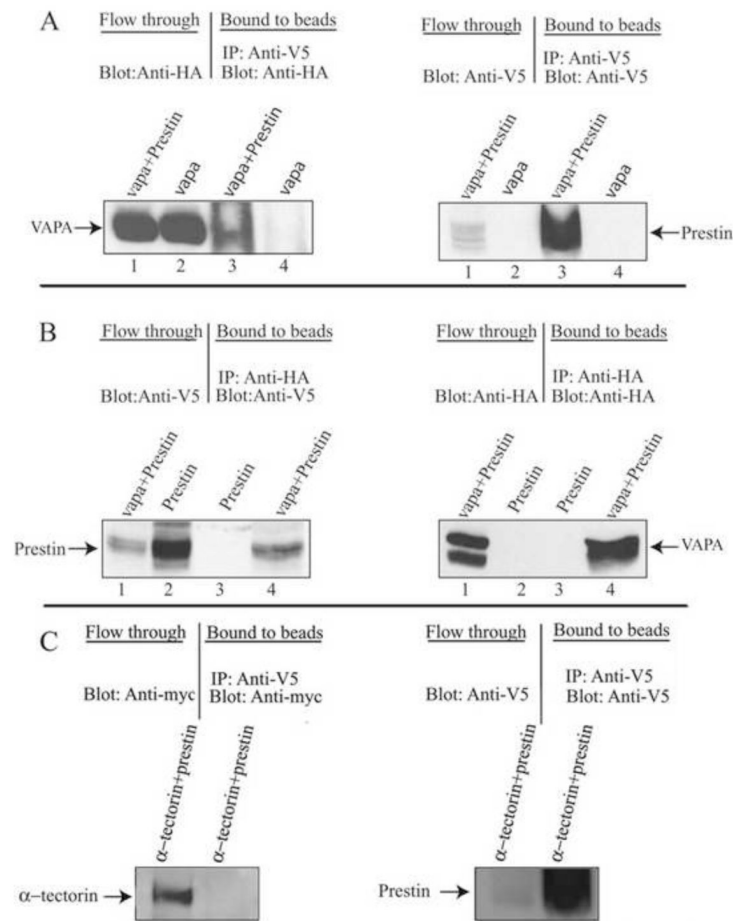
We thank Dr. W. Russin at the Biological Imaging Facility, Northwestern University for his help in image processing. We also thank Dr. Robert A. Lamb, Northwestern University, for providing mouse anti-HA antibody 12CA5. Dr. K. Legan and Dr. G. Richardson of the University of Sussex are thanked for providing the pBK\_NmycTecta plasmid. This work was supported by NIH Grants DC00089 to PD, DC006412 to JZ.

## REFERENCES

- [1]. Dallos P. The active cochlea. *J. Neurosci* 1992;12:4575–4585. [PubMed: 1464757]
- [2]. Ryan A, Dallos P. Effect of absence of cochlear outer hair cells on behavioural auditory threshold. *Nature* 1975;253:44–46. [PubMed: 1110747]
- [3]. Dallos P, Harris D. Properties of auditory nerve responses in absence of outer hair cells. *J. Neurophysiol* 1978;41:365–383. [PubMed: 650272]
- [4]. Harrison RV, Evans EF. Cochlear fibre responses in guinea pigs with well defined cochlear lesions. *Scand. Audiol. Suppl* 1979;83–92. [PubMed: 294692]
- [5]. Dallos, P.; Harris, DM.; Relkin, E.; Cheatham, MA. Two-tone suppression and intermodulation distortion in the cochlea: Effect of outer hair cell lesions. Delft University Press; 1980.
- [6]. Brownell WE, Bader CR, Bertrand D, de Ribaupierre Y. Evoked mechanical responses of isolated cochlear outer hair cells. *Science* 1985;227:194–196. [PubMed: 3966153]
- [7]. Santos-Sacchi J, Dilger JP. Whole cell currents and mechanical responses of isolated outer hair cells. *Hear. Res* 1988;35:143–150. [PubMed: 2461927]
- [8]. He DZ, Dallos P. Somatic stiffness of cochlear outer hair cells is voltage-dependent. *Proc. Natl. Acad. Sci. U. S. A* 1999;96:8223–8228. [PubMed: 10393976]
- [9]. Evans BN, Dallos P. Stereocilia displacement induced somatic motility of cochlear outer hair cells. *Proceedings of the National Academy of Sciences of the United States of America* 1993;90:8347–8351. [PubMed: 8378305]
- [10]. Zheng J, Shen W, He DZ, Long KB, Madison LD, Dallos P. Prestin is the motor protein of cochlear outer hair cells. *Nature* 2000;405:149–155. [PubMed: 10821263]
- [11]. Dallos P, Zheng J, Cheatham MA. Prestin and the cochlear amplifier. *J. Physiol* 2006;576:37–42. [PubMed: 16873410]
- [12]. Dallos P, et al. Prestin-based outer hair cell motility is necessary for mammalian cochlear amplification. *Neuron* 2008;58:333–339. [PubMed: 18466744]
- [13]. Liberman MC, Gao J, He DZ, Wu X, Jia S, Zuo Zuo, J. Prestin is required for electromotility of the outer hair cell and for the cochlear amplifier. *Nature* 2002;419:300–304. [PubMed: 12239568]
- [14]. Cheatham MA, Hheauynh KH, Gao J, Zuo J, Dallos P. Cochlear function in Prestin knockout mice. *J. Physiol* 2004;560:821–830. [PubMed: 15319415]
- [15]. Cheatham MA, et al. Evaluation of an independent prestin mouse model derived from the 129S1 strain. *Audiol. Neurootol* 2007;12:378–390. [PubMed: 17664869]
- [16]. Rajagopalan L, et al. Tuning of the outer hair cell motor by membrane cholesterol. *J. Biol. Chem* 2007;282:36659–36670. [PubMed: 17933870]
- [17]. Holley, MC. *The Cochlea: The Springer Handbook of Auditory Research*. Springer; New York: 1996.
- [18]. Zheng J, Du GG, Anderson CT, Keller JP, Orem A, Dallos P, Cheatham M. Analysis of the oligomeric structure of the motor protein prestin. *J. Biol. Chem* 2006;281:19916–19924. [PubMed: 16682411]
- [19]. Zheng J, Long KB, Matsuda KB, Madison LD, Ryan AD, Dallos PD. Genomic characterization and expression of mouse prestin, the motor protein of outer hair cells. *Mamm. Genome* 2003;14:87–96. [PubMed: 12584604]

- [20]. Zheng J, et al. The C-terminus of prestin influences nonlinear capacitance and plasma membrane targeting. *J. Cell. Sci* 2005;118:2987–2996. [PubMed: 15976456]
- [21]. Skehel PA, Martin KC, Kandel ER, Bartsch D. A VAMP-binding protein from *Aplysia* required for neurotransmitter release. *Science* 1995;269:1580–1583. [PubMed: 7667638]
- [22]. Nishimura Y, Hayashi M, Inada H, Tanaka T. Molecular cloning and characterization of mammalian homologues of vesicle-associated membrane protein-associated (VAMP-associated) proteins. *Biochem. Biophys. Res. Commun* 1992;254:21–26. [PubMed: 9920726]
- [23]. Skehel PA, Fabian-Fine R, Kandel ER. Mouse VAP33 is associated with the endoplasmic reticulum and microtubules. *Proc. Natl. Acad. Sci. U. S. A* 2000;97:1101–1106. [PubMed: 10655491]
- [24]. Wyles JP, McMaster CR, Ridgway ND. Vesicle-associated membrane protein-associated protein-A (VAP-A) interacts with the oxysterol-binding protein to modify export from the endoplasmic reticulum. *J. Biol. Chem* 2002;277:29908–29918. [PubMed: 12023275]
- [25]. Kawano M, Kumagai K, Nishijima M, Hanada K. Efficient trafficking of ceramide from the endoplasmic reticulum to the Golgi apparatus requires a VAMP-associated protein-interacting FFAT motif of CERT. *J. Biol. Chem* 2006;281:30279–30288. [PubMed: 16895911]
- [26]. Loewen CJ, Roy Roy, A, Levine TP. A conserved ER targeting motif in three families of lipid binding proteins and in Opi1p binds VAP. *Embo. J* 2003;22:2025–2035. [PubMed: 12727870]
- [27]. Wyles JP, Ridgway ND. VAMP-associated protein-A regulates partitioning of oxysterol-binding protein-related protein-9 between the endoplasmic reticulum and Golgi apparatus. *Exp. Cell. Res* 2004;297:533–547. [PubMed: 15212954]
- [28]. Teuling E, Ahmed S, Haasdijk E, Demmers J, Steinmetz MO, Akhmanova A, Jaarsma D, Hoogenraad CC. Motor neuron disease-associated mutant vesicle-associated membrane protein-associated protein (VAP) B recruits wild-type VAPs into endoplasmic reticulum-derived tubular aggregates. *J. Neurosci* 2007;27:9801–9815. [PubMed: 17804640]
- [29]. Ettayebi K, Hardy ME. Norwalk virus nonstructural protein p48 forms a complex with the SNARE regulator VAP-A and prevents cell surface expression of vesicular stomatitis virus G protein. *J. Virol* 2003;77:11790–11797. [PubMed: 14557663]
- [30]. Gkogkas C, Middleton S, Kremer AM, Wardrope C, Hannah M, Gillingwater TH, Skehel P. VAPB interacts with and modulates the activity of ATF6. *Hum. Mol. Genet* 2008;17:1517–1526. [PubMed: 18263603]
- [31]. Foster LJ, Weir ML, Lim DY, Liu Z, Trimble WS, Klip A. A functional role for VAP-33 in insulin-stimulated GLUT4 traffic. *Traffic* 2000;1:512–521. [PubMed: 11208137]
- [32]. Zheng J, Anderson CT, Miller KK, Cheatham M, Dallos P. Identifying components of the hair-cell interactome involved in cochlear amplification. *B.M.C. Genomics* 2009;10:127.
- [33]. Matsuda K, Zheng J, Du GG, Klocker N, Madison LD, Dallos P. N-linked glycosylation sites of the motor protein prestin: effects on membrane targeting and electrophysiological function. *J. Neurochem* 2004;89:928–938. [PubMed: 15140192]
- [34]. Cheatham MA, Zheng J, Huynh KH, Du GG, Gao J, Zuo J, Navarrete Navarrete, E, Dallos P. Cochlear function in mice with only one copy of the prestin gene. *J. Physiol* 2005;569:229–241. [PubMed: 16166160]
- [35]. Brunette DM, Till JE. A rapid method for the isolation of L-cell surface membranes using an aqueous two-phase polymer system. *J. Membr. Biol* 1971;5:215–224.
- [36]. Belyantseva IA, Adler HJ, Curi R, Frolenkov GI, Kachar B. Expression and localization of prestin and the sugar transporter GLUT-5 during development of electromotility in cochlear outer hair cells. *J. Neurosci* 2000;20:RC116. [PubMed: 11125015]
- [37]. Wu X, Gao J, Guo Y, Zuo J. Hearing threshold elevation precedes hair-cell loss in prestin knockout mice. *Brain. Res. Mol. Brain. Res* 2004;126:30–37. [PubMed: 15207913]
- [38]. Montcouquiol M, et al. Asymmetric localization of Vangl2 and Fz3 indicate novel mechanisms for planar cell polarity in mammals. *J. Neurosci* 2006;26:5265–5275. [PubMed: 16687519]
- [39]. Wang Y, Guo N, Nathans J. The role of Frizzled3 and Frizzled6 in neural tube closure and in the planar polarity of inner-ear sensory hair cells. *J. Neurosci* 2006;26:2147–2156. [PubMed: 16495441]

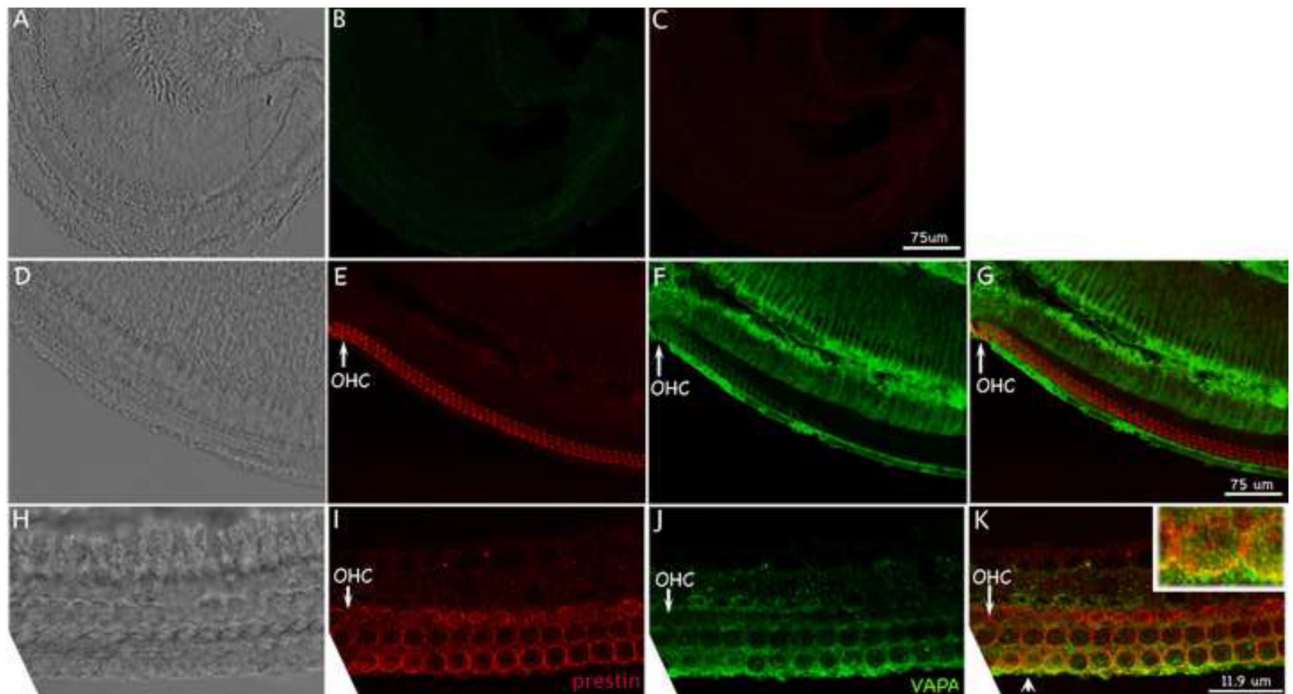
- [40]. Nagy I, Bodmer M, Schmid S, Bodmer D. Promyelocytic leukemia zinc finger protein localizes to the cochlear outer hair cells and interacts with prestin, the outer hair cell motor protein. *Hear. Res* 2005;204:216–222. [PubMed: 15925207]
- [41]. Zhang K, Kaufman RJ. Identification and characterization of endoplasmic reticulum stress-induced apoptosis in vivo. *Methods. Enzymol* 2008;442:395–419. [PubMed: 18662581]



**Figure 1.**

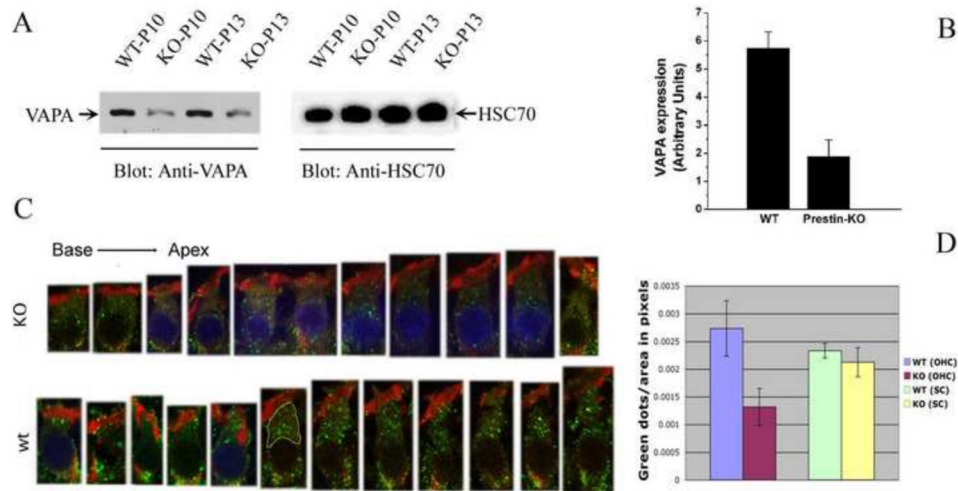
VAPA can specifically bind to prestin. HEK293T cell lysates from HA-VAPA and V5-prestin +HA-VAPA or V5-prestin and V5-prestin+HA-VAPA-expressing cells were subjected to co-IP with anti-V5 or anti-HA and Protein A sepharose, respectively. **A.** The co-IP of HA-VAPA and V5-prestin where VAPA was immunoprecipitated with V5-prestin and VAPA was visualized by anti-HA antibody. The presence of prestin in the eluate was also shown by staining with anti-V5 antibody. Lanes 1 and 2 show proteins from flow-through. Lanes 3 and 4 are eluates from prestin-anti-V5-beads. **B.** The co-IP of HA-VAPA and V5-prestin where prestin was immunoprecipitated with HA-VAPA and prestin was visualized by anti-V5 antibody. The presence of VAPA in the eluate was shown by staining with anti-HA antibody. Lanes 1 and 2 show proteins from flow-through. Lanes 3 and 4 are eluates from VAPA-anti-HA-beads. **C.** The negative control. The co-IP of myc- $\alpha$ -tectorin and V5-prestin shows that no  $\alpha$ -tectorin was present in the eluate from prestin-anti-V5-beads when blotted with anti-myc antibody whereas  $\alpha$ -tectorin protein is present in the flow-through. The presence of prestin in the eluate was shown by staining with anti V5 antibody.



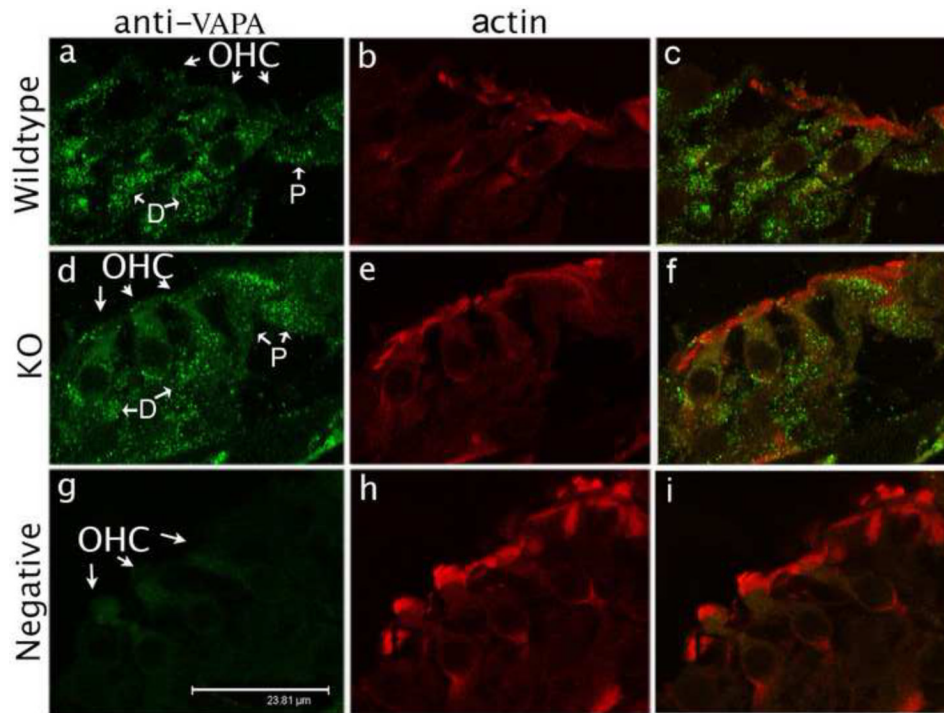


**Figure 2.**

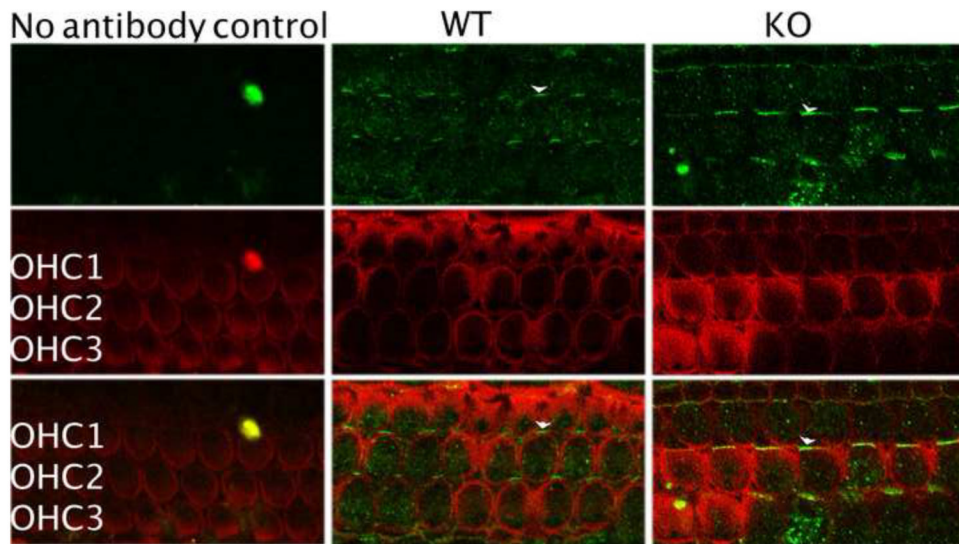
VAPA and prestin co-localize in OHCs. **A-C**: Images of negative controls: no primary antibodies were added. **D-G**: The same group of cells with prestin staining (**E**), VAPA staining (**F**), and the corresponding phase-contrast image (**D**) of a whole-mount sample show a cross section of the organ of Corti. **G** shows superimposed images of **E** and **F**. **H-K**: The same group of OHCs with prestin staining (**I**), VAPA staining (**J**) and the corresponding phase-contrast image (**H**) of a whole-mount sample. In **K** images of **I** and **J** are superimposed. Co-localization of VAPA and prestin staining appears in yellow color as indicated by an arrowhead. The image corresponding to the location marked with the arrowhead is given at higher magnification for better examination (right corner). Red: anti-mPres staining. Green: anti-VAPA staining. **A-G**: low magnification images: Bar length: 75  $\mu\text{m}$ . **H-K**: high magnification images: Bar length: 11.9  $\mu\text{m}$ . Cochlear samples were collected from P5 WT-mice.

**Figure 3.**

The expression of VAPA protein is higher in OHCs derived from WT- than from prestin-KO mice. **A.** Western blot data collected from P10 and P13 cochleae derived from WT- and prestin-KO mice. **B.** Semi-quantitative analysis of VAPA proteins in WT- and prestin-KO mice. Intensities of VAPA protein bands were divided by band intensities of house-keeping protein HSC70. WT cochlea: n=2, prestin-KO cochlea: n=2 (p=0.01). **C.** Images of individual OHCs (P13) selected from different locations, either WT-(bottom row) or prestin-KO (top row) mice. **D.** Quantification of VAPA-staining vesicles (green spots) in WT- and prestin-KO OHCs and supporting cells. The areas between cuticular plates and nuclei, as indicated by a yellow border in one of the WT OHCs in **C**, were selected and measured using NIH Image J software. More green spots are observed in OHCs from WT-mice, independent of cochlear location. In fact, there is a statistical difference between WT-OHCs and prestin-KO-OHCs (p=0.0001; n=13), with WT-OHCs having more VAPA-green dots per area. The blue staining of some nuclei is due to the mounting of these samples in Vectashield containing DAPI. Other samples, mounted in Fluoromount-G without the DAPI dye, have unstained nuclei. A fixed area in supporting cells of WT- and KO-organ of Corti were selected for counting green spots. In supporting cells, no significant difference (p=0.65) was found in VAPA expression between WT- and KO-cochlea. Green: anti-VAPA. Red: Texas Red-X phalloidin labeling actin.

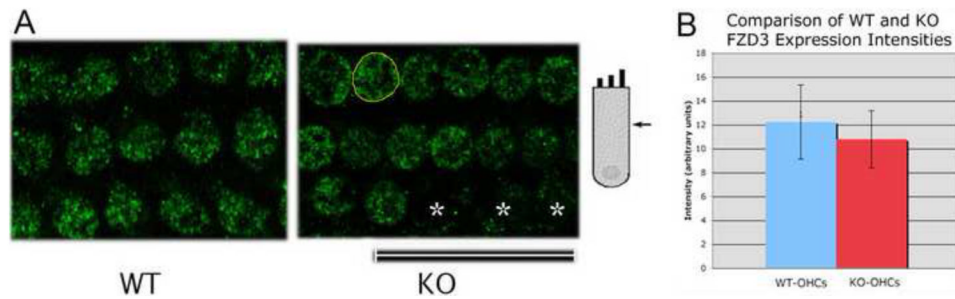


**Figure 4.** VAPA expression in the organ of Corti at P13. VAPA staining (anti-VAPA, green spots) is present in OHCs and in supporting cells in both WT (**a**) and prestin-KO (**d**) mice. However, punctate VAPA staining is absent in the negative control (**g**), which is not stained with anti-VAPA primary antibody, but stained with secondary antibody and Texas Red-X phalloidin. Actin (Texas Red-X phalloidin) expression is similar in WT (**b**), KO (**e**) and in the negative control (**h**). The right column (**c**, **f**, **i**) shows superimposed images of first two columns. Bar length: 23.8  $\mu\text{m}$ . D: Deiters' cells, P: pillar cells.



**Figure 5.**

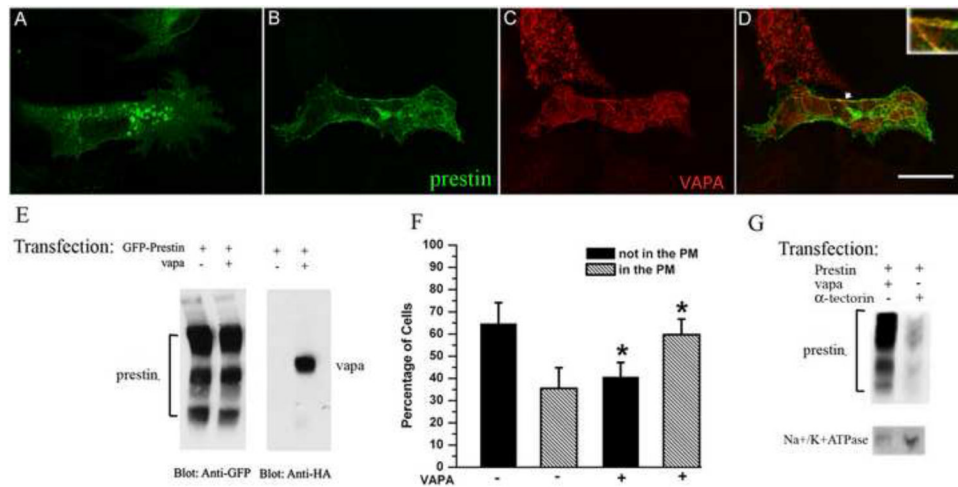
No difference in FZD3 expression from WT- and prestin-KO mice at P0. FZD3 (anti-FZD3, green) is asymmetrically located only at one side of the OHC's proximal edge as indicated by white arrowheads in both WT and prestin-KO samples. The level and pattern of FZD3 expression are virtually the same for WT and KO cells. However, at this stage of development, there is no prestin protein in OHCs. Actin is stained with Texas Red-X phalloidin (red).



**Figure 6.**

Adult OHCs show no difference in FZD3 expression in WT and prestin-KO mice. **A.** FZD3 (anti-FZD3, green) is located in the cytoplasm of both WT and prestin-KO OHCs. No asymmetrical expression is found in adult OHCs. **B.** Mean fluorescent intensities of FZD3 staining in the cytoplasmic areas of WT- and KO-OHCs outlined in yellow. Average fluorescence intensity in arbitrary units per cell for WT-OHCs is about 12 (12.2, SD: 3.1), for KO-OHCs about 11 (10.78, SD: 2.39). There is no statistical difference between WT-OHCs and KO-OHCs ( $p=0.11$ ,  $N=15$  for WT and 14 for KO). Missing OHCs are indicated by an asterisk. Bar length: 23.8  $\mu\text{m}$ .



**Figure 7.**

Prestin distribution patterns under the influence of VAPA. OK cells were transiently transfected with GFP-prestin alone (**A**) or co-transfected with GFP-prestin+HA-VAPA (**B**, **C**). Approximately 28 hrs post transfection, cells were fixed and incubated with anti-HA antibody followed by the corresponding secondary antibody. The yellow image (right column) is superimposed from green and red images, indicating the partial co-localization of prestin and VAPA (**D**) as indicated by the arrow. For better visualization of the co-localization, the co-localization portion is shown in the right corner at higher magnification. Bar length: 23.8  $\mu$ m. **A** shows that prestin is intracellularly localized in the absence of over-expressed VAPA, whereas in the presence of over-expressed VAPA (**B**) prestin is localized to the plasma membrane. **E**. Comparison of GFP-prestin expression in OK cells transfected with GFP-prestin alone or co-transfected with GFP-prestin+HA-VAPA. GFP-prestin expression was similar in both GFP-prestin- and GFP-prestin+HA-VAPA transfected cells where GFP-prestin was visualized using anti-GFP antibody. VAPA was observed using anti-HA antibody. **F**. Distribution of prestin protein under the influence of VAPA. OK cells were transfected with either the plasmid encoding GFP-prestin, or plasmids encoding GFP-prestin+VAPA. OK cells with green staining (prestins) in the PM were defined as “in the PM” (hatched bars). OK cells without green staining in the PM were defined as “not in the PM” (black bars). **G**. More prestin is delivered to the PM in the presence of over-expressed VAPA than in presence of a control protein,  $\alpha$ -tectorin. GFP-prestin was visualized by anti-GFP. Na<sup>+</sup>/K<sup>+</sup>ATPase, which is a PM marker, was stained with anti-Na<sup>+</sup>/K<sup>+</sup>ATPase.